

# We are IntechOpen, the world's leading publisher of Open Access books Built by scientists, for scientists

4,800

Open access books available

122,000

International authors and editors

135M

Downloads

Our authors are among the

154

Countries delivered to

TOP 1%

most cited scientists

12.2%

Contributors from top 500 universities



WEB OF SCIENCE™

Selection of our books indexed in the Book Citation Index  
in Web of Science™ Core Collection (BKCI)

Interested in publishing with us?  
Contact [book.department@intechopen.com](mailto:book.department@intechopen.com)

Numbers displayed above are based on latest data collected.  
For more information visit [www.intechopen.com](http://www.intechopen.com)



---

## Development, Characterization, and Applications of Capsaicin Composite Nanofiltration Membranes

---

Jesús Álvarez-Sánchez,  
Griselda Evelia Romero-López, Sergio Pérez-Sicairos,  
German Eduardo Devora-Isiordia,  
Reyna Guadalupe Sánchez-Duarte and  
Gustavo Adolfo Fimbres-Weihs

Additional information is available at the end of the chapter

<http://dx.doi.org/10.5772/intechopen.76846>

---

### Abstract

Biofouling in reverse osmosis (RO) membranes is a severe problem, causing a decrease in both permeate flux and salt rejection and increasing transmembrane pressure. Capsaicin extract inhibits bacterial growth and is therefore used in this study to prepare a thin-film composite membrane and membrane support. Four types of nanofiltration (NF) membranes were prepared by interfacial polymerization onto a porous support prepared by the phase inversion method. Membrane A was the control membrane with no capsaicin extract, membrane B contains capsaicin in the polyamide thin film, membrane C contains capsaicin in the porous support, and membrane D contains capsaicin in both the thin film and support layers. Three different salts ( $\text{Na}_2\text{SO}_4$ ,  $\text{MgSO}_4$ , and  $\text{NaCl}$ ) were used at different concentrations (1000, 3000, and 5000 ppm) to test the performance of the membranes in terms of salt rejection and permeate flux. Membrane B showed the highest rejection for all the salts and concentrations tested. For 5000 ppm  $\text{NaCl}$ , the permeate flux for membrane B was 14.81% higher, and salt rejection was 19.6% higher than membrane A. Future work will evaluate the anti-biofouling properties of the membranes prepared with capsaicin, when exposed to seawater microorganisms.

**Keywords:** nanofiltration membrane, capsaicin, characterization, atomic force microscopy, contact angle, reverse osmosis

---

## 1. Introduction

The capability of several human activities, like industry and mining, has expanded throughout the last decades [1], which has led to a similar pace of improvements in membrane technology for separation. Drinking water treatment processes have developed to the point of requiring more advanced pretreatment processes [2]. Nanofiltration (NF) might function as a pretreatment for reverse osmosis desalination [3], as it can remove hardness, specific heavy metals, and reduce the salt content of feed water [4].

In addition, one of the main problems faced by desalination processes is the inevitable appearance of biofouling on its membranes [5, 6]. This causes problems such as decreases in permeate flux and salt rejection, as well as an increase in transmembrane pressure [7]. In an effort to reduce the most damaging effects of biofouling, there have been many studies for testing numerous anti-fouling agents and solutions added during membrane fabrication. However, not all these attempts include organic-based preparation, suggesting that there may be possible hazards for human health, after consumption [8, 9]. Pepper extract, the source of the capsaicin molecule, has proven to limit bacterial growth [10]; therefore, its addition during the membrane fabrication process may help control biofilm formation on the membrane surface.

In this study, nanofiltration membranes were prepared (**Figure 1**) for brackish water treatment. It is desirable for the desalination membranes to have hydrophilic properties, as this usually correlates with the tendency of a membrane for allowing water to permeate instead of rejecting it (hydrophobic) [11]. Contact angle measurements are usually carried out to determine the degree of hydrophilicity or hydrophobicity of a surface [12]. This study includes an analysis of the fabrication, as well as the characterization of four nanofiltration membranes, before and after their performance testing on a cross-flow module, operated with an aqueous salt solution to determine salt rejection. Membrane characterization is also performed through atomic force microscopy (AFM) and attenuated total reflectance infrared spectroscopy (ATR-IR) [13]. Membranes prepared with capsaicin will later be assessed for their anti-biofouling properties, to evaluate whether they are resistant to biofouling by seawater microorganisms.

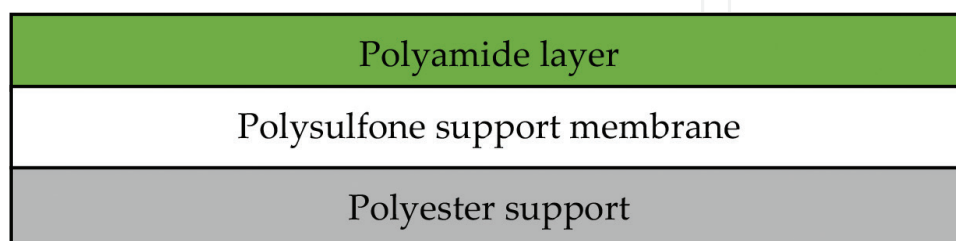


**Figure 1.** Scheme of composite membrane.

## 2. Methodology

### 2.1. Polymers and monomers

Polysulfone (PS purity > 99%), polyether sulfonyl (PES; purity > 99%), piperazine (PP; purity > 99%), and 1,3,5-Benzenetricarbonyl chloride (TMC; purity > 98%) were obtained from Sigma-Aldrich. Chiltepin pepper extract [9] (capsaicin extract) was obtained in the laboratory as a source of the capsaicin molecule (**Figure 2**). This extract was used to prepare nanofiltration membranes.

To corroborate the extraction of capsaicin, infrared spectroscopy was performed, showing the following signals:

- tension vibration for N-H present on the amide group, shown at  $3381.8\text{ cm}^{-1}$ ; this signal hides within the O-H functional group, which has a range from  $3400$  to  $3200\text{ cm}^{-1}$ ;
- vibration departing from tension on C-H at alkene located at  $3010.36\text{ cm}^{-1}$ ;
- C-H vibration corresponds to methylene alkanes, at  $2924.8\text{ cm}^{-1}$ ;
- methylene symmetrical tension for C-H present at  $2853.77\text{ cm}^{-1}$ ;
- vibration through tension for C = O for the amide group at  $1744.74\text{ cm}^{-1}$ ;
- vibration through stretching on C = O of the amide group at  $1652.78\text{ cm}^{-1}$ ;
- vibration through the asymmetrical bending of  $\text{CH}_2$  at  $1464.28\text{ cm}^{-1}$ ;
- the signal at  $1374.7\text{ cm}^{-1}$ , corresponding to a  $\text{CH}_3$  bending; and
- an asymmetrical deformation of  $\text{CH}_2$  at  $721.66\text{ cm}^{-1}$ .

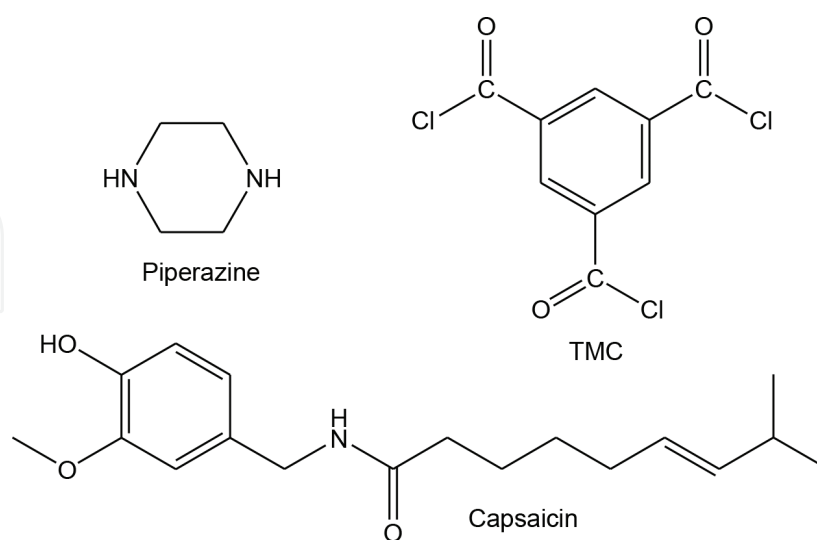


**Figure 2.** Chemical structure of the monomers for preparation nanofiltration composite membranes: piperazine, capsaicin and 1,3,5-benzenetricarbonyl chloride (TMC).

## 2.2. Preparation of the microporous polysulfone membrane

Sheets of microporous polysulfone membrane supports were prepared, following the methodology by Perez-Sicairos et al. [14] and Lin et al. [15]. Four sheets were prepared through a phase inversion process; a polymer solution including 18% w/w of dried polysulfone (12 g) was dissolved in a mixed solvent of n-methyl-pyrrolidone (NMP, 82 g) and an independent addition of sulfonated polysulfone (6 g), inside a clear jar and sealed with a Teflon cap. This glass bottle was subjected to a rotator device, spinning at 52 rpm under a heating light, to achieve a homogeneous polymer solution. A 71 × 28 cm Holytek paper piece (0.12 mm thick) was cut and held onto the membrane casting machine, where the polymeric solution was spread through the casting blade, allowing a solution spreading to a depth of 0.004 mm. Submersion speed was set at full capacity (11 m/min). The tank was filled with distilled water, providing a bath to induce phase inversion and a resting pace for 6 min. Finally, the membranes proceeded to a rinsing stage with distilled water for 2 min, in order to eliminate the excess of floating polymer.

## 2.3. Preparation of nanofiltration membranes with capsaicin

Nanofiltration membrane production started with the preparation of porous polysulfone membrane via the phase inversion method, as reported by [14, 15]. The NF membrane was prepared by interfacial polymerization, over the porous polysulfone membrane. Two chemical solutions were prepared, an aqueous solution containing piperazine (solution A) and an organic solution containing 1, 3, 5 benzene-tricarbonyl trichloride (TMC). The composition of each of these solutions was as follows. The composition of the aqueous solution (A) was piperazine (0.25% w/w), polyvinyl alcohol (0.25% w/w), and sodium hydroxide (0.5% w/w). This solution was prepared as follows: for each 250 g of solution A, 1.25 g of sodium hydroxide were weighed and placed inside a 250 mL flask, with 100 mL of distilled water. The preparation was stirred. Moreover, 0.63 g of polyvinyl alcohol was added until full dilution. Then, 0.63 g of piperazine was added to the flask and filled to 250 mL. The composition of the organic solution (solution B) was TMC (1.0% w/w) and hexane. To prepare it, the procedure was as follows: for each 250 mL of solution B, 1 g of capsaicin extract and 1.5 g of TMC were weighed and the solution was filled to 250 mL with hexane. The first of the membranes, labeled control, was prepared from solution A and solution B.

In order to prepare the experimental membranes with distinctive characteristics, capsaicin extract was added during the preparation process, using four different concentrations, as shown in **Table 1**.

Membrane	Support layer	Composite layer	Capsaicin (g)
A	Polysulfone	Polyamide	0
B	Polysulfone	Polyamide + capsaicin	1
C	Polysulfone + capsaicin	Polyamide	1
D	Polysulfone + capsaicin	Polyamide + capsaicin	2

**Table 1.** Composition for nanofiltration membrane preparation.

Once the porous support for the membranes was prepared, two of the pieces were designated as composite membranes. These membranes received the concentrations shown in **Table 2**.

## 2.4. Characterization of nanofiltration membranes

### 2.4.1. Atomic force microscopy

Atomic force microscopy (AFM) was performed with a PS 50–50-15 (50  $\mu\text{m}$ ) scanning probe microscope instrument (AFM workshop) to determine the surface morphology of the nanofiltration membrane. The software Gwyddion 2.4 was used to obtain 3D images and roughness measurements (root mean square, RMS). A sample size of  $0.5 \times 0.5$  cm was used to analyze the nanofiltration membranes.

### 2.4.2. Attenuated total reflectance infrared spectroscopy

Attenuated total reflectance infrared (ATR-IR) characterization of the nanofiltration membrane surface was carried out with a Nicolet iS5 Fourier transform infrared spectrometer and the accessory iD3 ATR (thermo Fisher scientific). For ATR-IR analysis of the nanofiltration membranes samples, a germanium crystal was employed. A sample size of  $0.5 \times 0.5$  cm was used to analyze the nanofiltration membranes.

### 2.4.3. Contact angle

Contact angle measurements were performed with a dataphysics contact angle system (OCA15SEC), camera iDs and injection system ES. A sample size of  $3 \times 2$  cm was used to analyze the nanofiltration membranes. The water used was previously distilled and filtered (0.2  $\mu\text{m}$ ). The water drop was placed on different locations on the membrane surface, at a temperature of 22°C.

### 2.4.4. Cross-flow equipment

The operation of the cross-flow cell unit (**Figure 3**) was as follows. Starting from a 20 L feed tank, the feed solution (NaCl,  $\text{MgSO}_4$ , and  $\text{Na}_2\text{SO}_4$  at the different concentrations) is conducted

Membrane	Polysulfone support			Polyamide layer		
	Polysulfone (g)	Sulfonated polysulfone (g)	Capsaicin (g)	Trimesoyl chloride (mL)	Piperazine (mL)	Capsaicin (g)
A	12.0	6.0	NA	100	0.25	NA
B	12.0	6.0	NA	100	0.25	1
C	11.5	5.5	1	100	0.25	NA
D	11.5	5.5	1	100	0.25	1

**Table 2.** Polysulfone and polyamide composition.

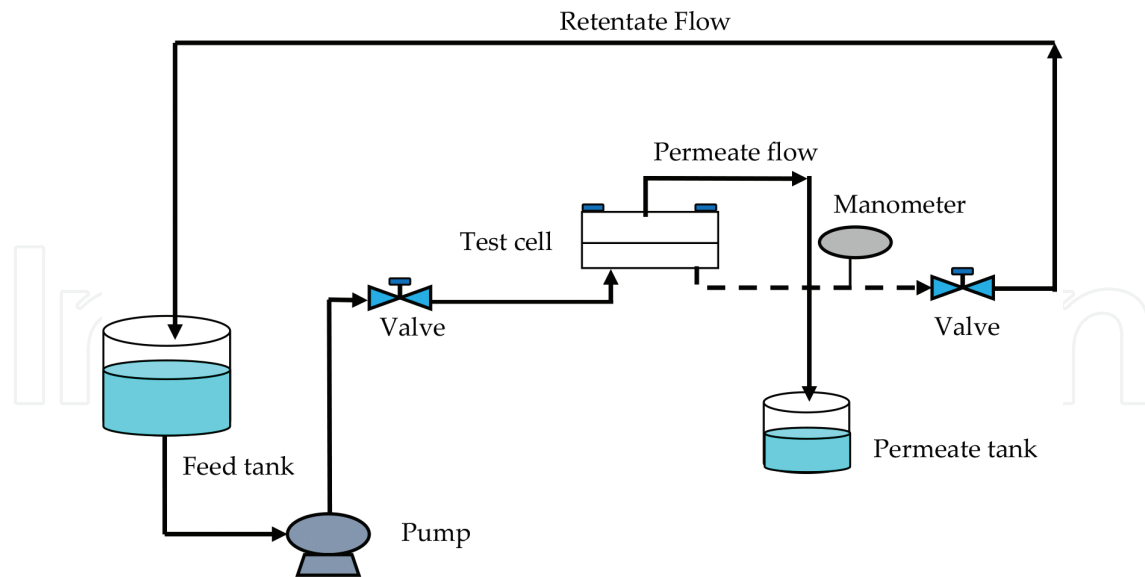


Figure 3. Cross-flow equipment for membrane testing.

to the cross-flow cell, with an applied and stable pressure (80 psi). A  $3.5 \times 2$  membrane piece is placed in the interior of the cell. Once feed water reaches the membrane cell, two outcomes occur: some water permeates through the membrane, leaving impurities behind and producing purified water, and the rest of the water that does not cross the membrane flows to a retentate tank. This latter effluent will have a distinctive characteristic of higher salinity than the feed flow.

The thickness of the membranes was measured using a micrometer (Holytex paper 0.12 mm). This information can be related to the uniformity of the membrane surface. Finally, the salt rejection by the membrane is calculated considering the conductivity in the feed flow and in the permeate flow (after 60 min). For concentrations in the range of different salts used, the conductivity is proportional to solution concentration, so salt rejection can be determined using the following equation:

$$\% \text{Conductivity rejection} = \frac{\Omega_0 - \Omega_{60}}{\Omega_0} \times 100\% \quad (1)$$

where  $\Omega_0$  represents the conductivity of the feed and  $\Omega_{60}$  represents conductivity of the permeate after 60 min of permeation. In terms of concentration, the rejection percentage is given by:

$$\%R = \frac{C_f - C_p}{C_f} \times 100\% \quad (2)$$

where  $\%R$  is salt rejection,  $C_f$  is the concentration of salt in the feed, and  $C_p$  is the concentration of salt in the permeate.

### 3. Results and discussion

#### 3.1. Test on cross-flow equipment

The data in **Figure 4** point to a decrease in permeate flux as the salt concentration increases. This can be appreciated for the three salts tested ( $\text{Na}_2\text{SO}_4$ ,  $\text{MgSO}_4$ , and  $\text{NaCl}$ ) under constant pressure (80 psi). Comparing the control membrane A with the rest of the membranes that include capsaicin in their formulation, it is observed that capsaicin addition tends to increase permeate flux.

For the  $\text{NaCl}$  solution at 1000 ppm, membrane B presented a permeate flux increase of 9.1% compared to membrane A, whereas at 5000 ppm, the increase was 14.81%. Membrane B presented the highest permeate flux increment, with membranes C and D also having permeate flux increases compared to membrane A but not as high as those of membrane B.

Due to the hydrophilic properties of capsaicin, the flux increments observed can be attributed to the capsaicin present in the membrane elaboration process for membranes B, C, and D. The capsaicin molecule has two main functional groups: hydroxyl, a polar group which presents affinity to water, and amide, which has nitrogen and a couple of free electrons generating polarity, also resulting in affinity to water. Hence, both characteristics result in hydrophilic properties on the membrane surface.

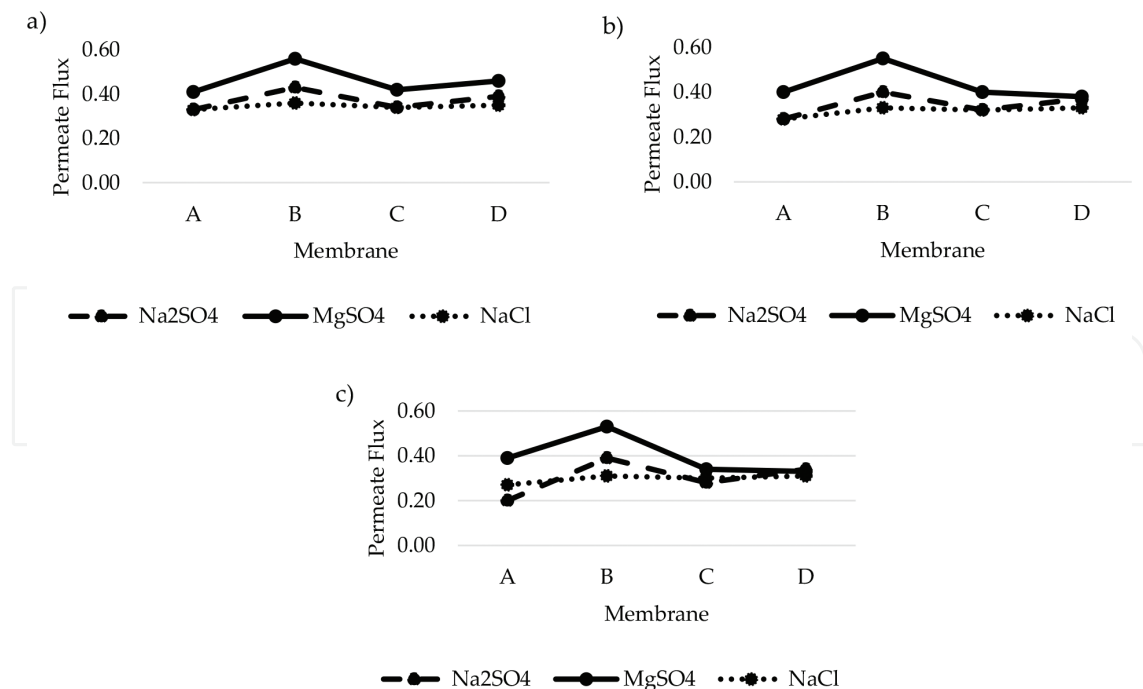


**Figure 4.** Permeate flux results for the membranes, with  $\text{Na}_2\text{SO}_4$ ,  $\text{MgSO}_4$  and  $\text{NaCl}$  solutions at (a) 1000, (b) 3000 and (c) 5000 ppm respectively.



Even more important than its ability to permeate the main function of a membrane is to separate undesired impurities from water, that is, their salt rejection. All the membranes were tested using an NaCl solution at different concentrations (1000, 3000, and 5000 ppm) with the results shown in **Figure 5**. For each of these concentrations, the membranes show a very similar trend: membrane A (blank) has less salt removal in relation to membrane D. Membrane C shows less rejection than every other membrane (**Table 3**).

The membranes that include capsaicin extract also present a higher salt rejection than the control membrane. Membrane D presented the highest salt rejection. A possible reason of this greater NaCl rejection is the content of capsaicin placed on the support layer (polysulfone) or on the active layer (polyamide). The capsaicin functional groups having free electrons provoke major NaCl rejections. Membrane B also presented a significant increase in salt rejection compared to the control membrane A.

### 3.2. Characterization by atomic force microscopy

Atomic force microscopy allows us to zoom into a small area of the membrane surface. Using this technique, the roughness of the membrane can be visualized, providing measurement data in the scale of microns. Membrane roughness affects both the permeate flux and the salt rejection. Furthermore, roughness provides spaces for marine bacteria to settle, initiating biofilm formation, which later leads to membrane biofouling. For these reasons, smooth surfaces are most desirable on membranes.

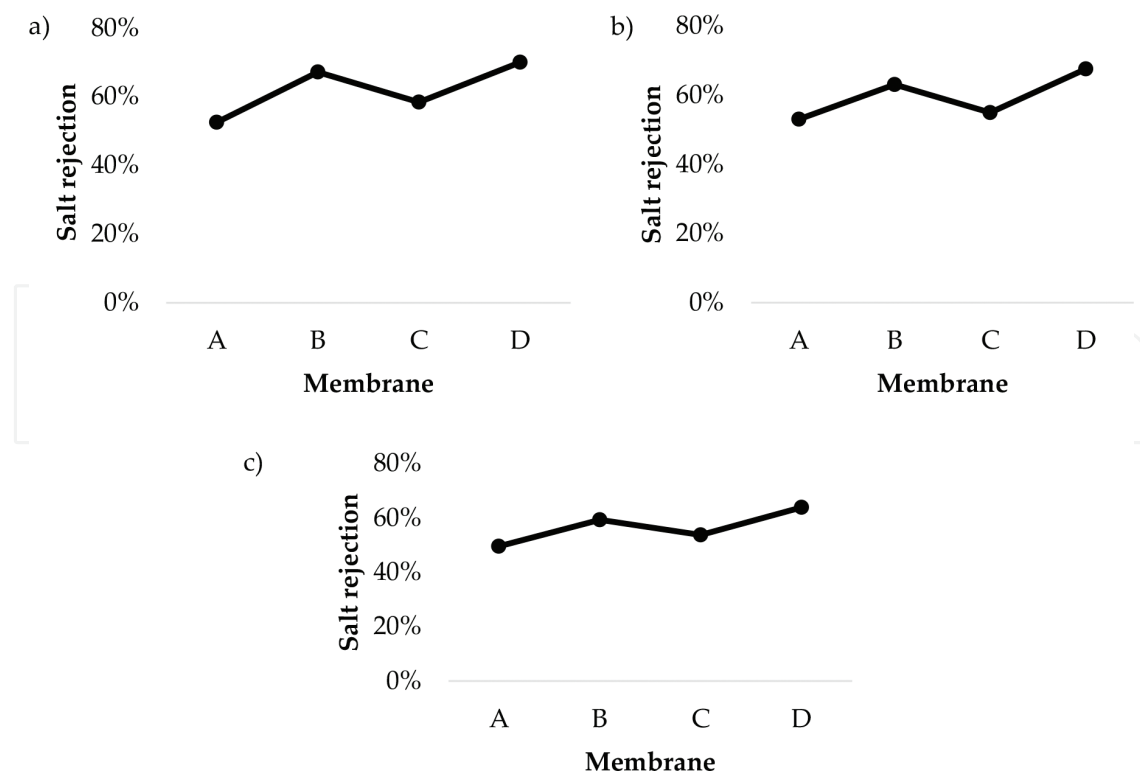


**Figure 5.** Salt rejection results for the membranes, with NaCl solutions at (a) 1000, (b) 3000 and (c) 5000 ppm respectively.

NaCl (ppm)	A (%)	B (%)	C (%)	D (%)
1000	52.5	67.22	58.41	70.06
3000	53.05	63.09	55.00	67.62
5000	49.59	59.30	50.98	63.92

**Table 3.** NaCl rejection percentage for membranes A, B, C, and D.

Atomic force microscopy was performed (**Figure 6**) in order to characterize the surface of the membranes. A scale of 50  $\mu\text{m}$  was used, such that the scanned area was 2500  $\mu\text{m}^2$  for each membrane. Each membrane was measured at five different points. The RMS roughness measurements for each membrane, as well as the average measurements, are presented in **Table 4**.

From **Table 4**, it is evident that adding capsaicin extract to the active layer reduces the average roughness from 334.08 (membrane A) to 129.4 nm (membrane B). Similarly, when capsaicin was added to both the active layer and the porous support, the average roughness decreased from 334.08 (membrane A) to 221.26 nm (membrane D). On the other hand, the membrane with capsaicin only in the porous support (membrane C) presented the smallest reduction in average roughness, from 334.08 (membrane A) to 276.66 nm (membrane C). This suggests that including capsaicin on the polyamide active layer reduces the surface roughness the membranes.

### 3.3. Characterization by contact angle measurement

The contact angle measurement calculates the angle formed between the surface of a water droplet and a solid surface (see **Figure 7**). This measurement is related to the wettability. In

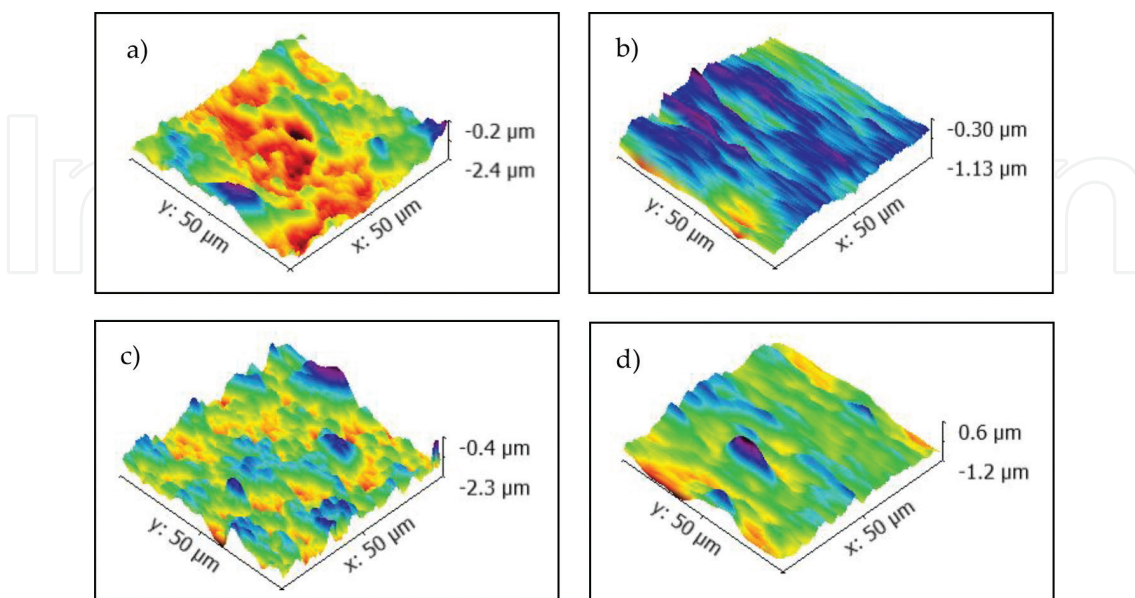


**Figure 6.** Atomic force microscope images and measurements for membranes A, B, C and D.

Membrane	AFM Measurement of RMS roughness (nm)					Average RMS roughness (nm)
A	306.2	325.5	357.8	318.8	362.1	334.08
B	97.4	108.8	176.6	100.0	164.2	129.39
C	294.2	305.1	264.9	245.7	273.4	276.66
D	266.2	203.7	185.5	199.1	251.8	221.26

**Table 4.** Membrane roughness values from AFM measurements.

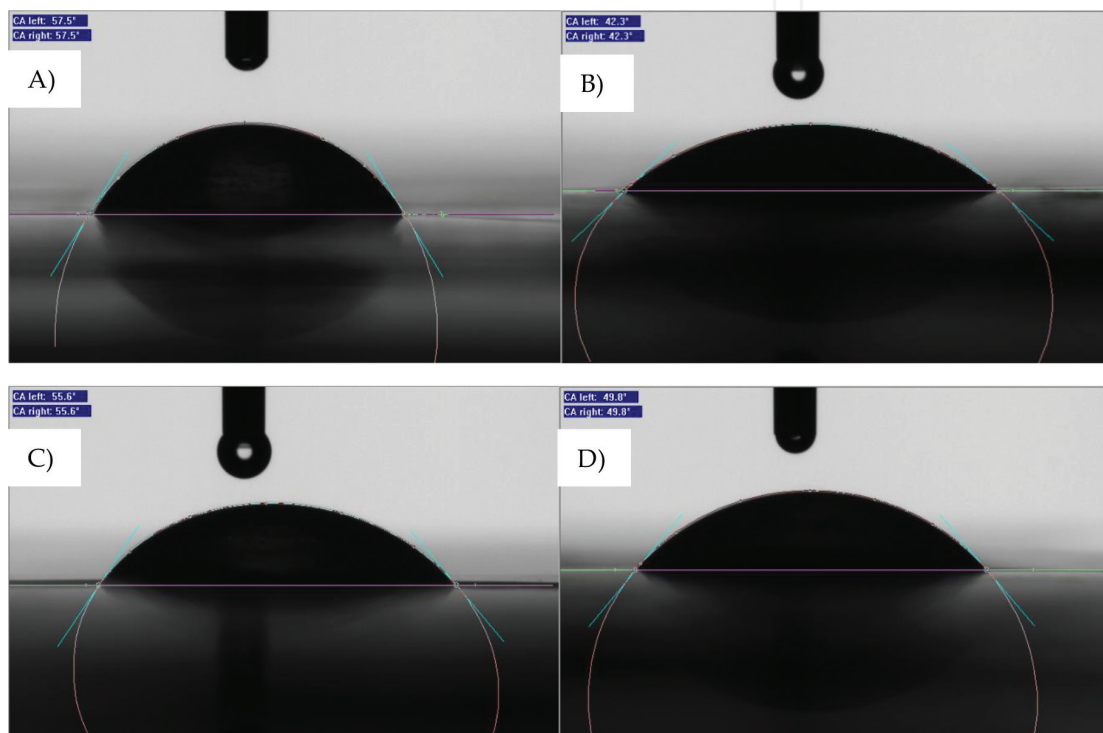


**Figure 7.** Contact angle measurements for membranes A, B, C and D.

the case of membranes, it can also be related to the permeability of the membrane, as a smaller angle means that water can dissolve more readily in the membrane matrix. Every liquid, at a given temperature, will show a unique equilibrium contact angle.

**Table 5** shows contact angle measurements for the membranes tested, at an ambient temperature of 22°C. The control membrane A had the largest contact angle and membrane B presented the smallest. The lower contact angles exhibited by membranes B and D may be attributed to the presence of capsaicin on the surface of those membranes. This is also supported by the permeate flux results, as membranes B and D resulted in the highest values for flux. Moreover, it was also found that the inclusion of capsaicin in the porous support layer of the membrane (membrane C) also leads to a smaller contact angle than the control membrane A, albeit to a lesser degree than when capsaicin is included in the active layer.

Membrane	Description	Measurement					
		1	2	3	4	5	Average
A	PS-TMC	56.8	57.5	59.5	58.6	57.0	57.88
B	PS-TMCCAP	34.9	42.3	40.7	38.1	34.4	38.08
C	PSCAP-TMC	55.0	55.6	52.1	53.5	54.9	54.22
D	PSCAP-TMCCAP	48.1	47.3	49.8	47.2	49.1	48.30

Table 5. Contact angle measurements for membranes.

### 3.4. Characterization by ATR-IR

The infrared spectra for the four membranes are shown in **Figure 8**. The spectra for membranes A and C do not show vibration through stretching on C=O of the amide group at 1652.78 cm<sup>-1</sup>. This is due to the absence of capsaicin in membrane A, while membrane C only included capsaicin in the porous support layer and, therefore, the infrared spectrum is not able to detect it. On membrane B, the signal is found at 1605.97 cm<sup>-1</sup> and for membrane D at 1619.90 cm<sup>-1</sup>.

It is possible that the signal at 1652.78 cm<sup>-1</sup> was not seen due to a new link formed between capsaicin and the acyl on TMC, developing a new covalent link between a carbonyl group and

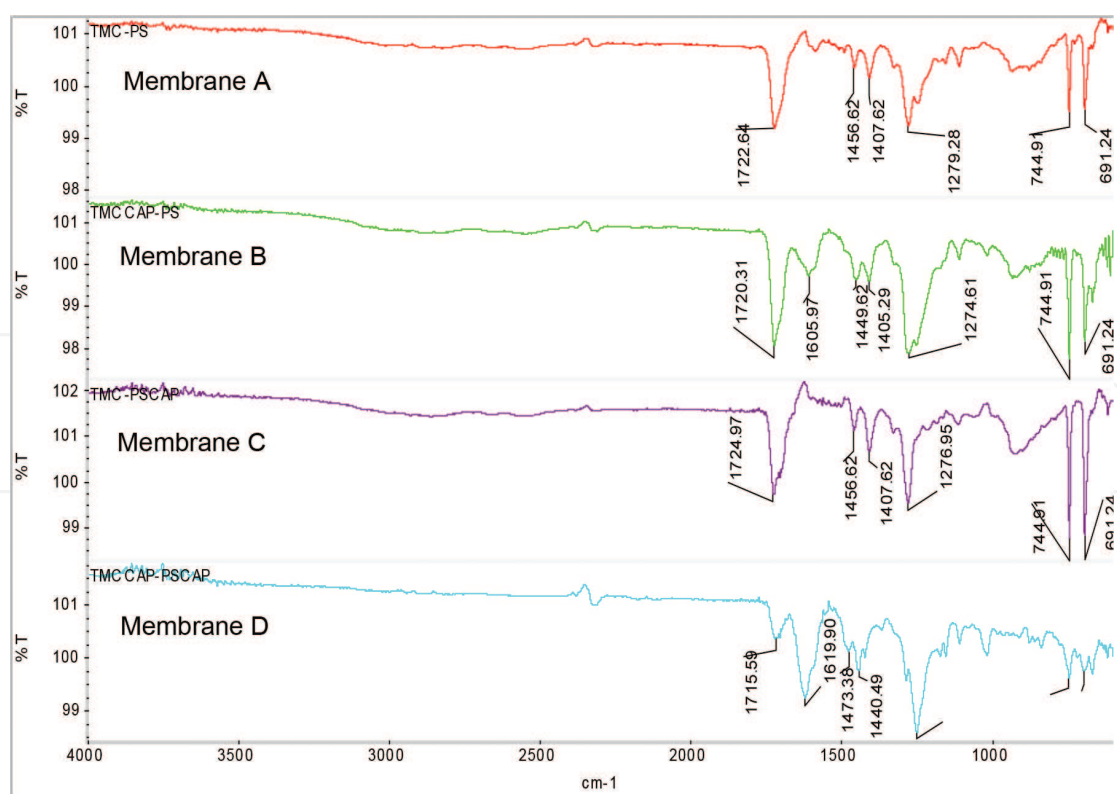
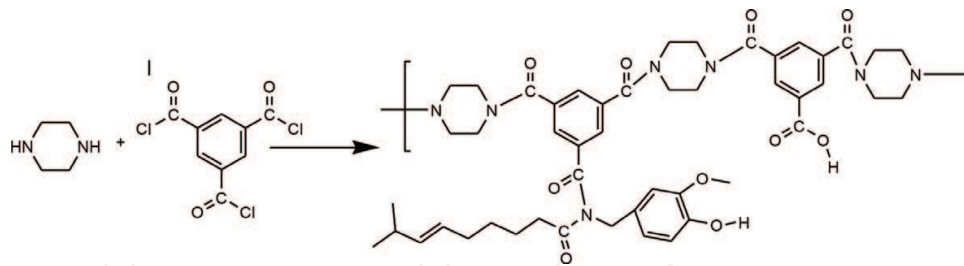


Figure 8. Infrared spectra for membranes A, B, C and D.



**Figure 9.** Piperazine – 1,3,5 Benzenetricarbonyl trichloride – capsaicin reaction.

nitrogen on the amide of capsaicin. Then, a new functional group is formed:  $\text{Ar-C(=O)-N-C(=O)}$  (**Figure 9**). The wavelength for this new link would be lower, because of the resonance effect of the free electrons of nitrogen, generating a simple C-O link, as Pavian et al. [16] had expressed.

#### 4. Conclusions

Nanofiltration membranes including capsaicin were prepared and characterized through contact angle measurements, AFM, ATR infrared spectroscopy and cross-flow tests. The ATR infrared spectroscopy showed that capsaicin reacted with the TMC, forming a new covalent link, which did not exist in the control membrane without capsaicin. In addition, AFM imaging showed that the surface of membranes with capsaicin in the active layer presented reduced roughness compared to the control membrane.

The results presented in this chapter show that capsaicin-based composite membranes present higher hydrophilic characteristics than traditional composite membranes. These properties of the capsaicin molecule can be attributed to its hydroxyl and amide groups, resulting in affinity to water. The hydrophilic character of the membranes with capsaicin was also reflected higher water permeability by the membranes.

It was also found that higher hydrophilicity and permeability could mostly be attributed to capsaicin present on the active layer of the membranes. This is because the presence of capsaicin in the porous membrane support layer did not show significant flux increases. Although capsaicin in the porous support increased salt rejection, we concluded that the application of capsaicin on the support layer of the membrane is not necessary. It is expected that nanofiltration membranes with capsaicin will result in better anti-biofouling properties than typical commercial membranes and, therefore, their service life would be longer. Future work will test this hypothesis.

#### Acknowledgements

The authors acknowledge project funding provided by PROMEP, CONACYT and the Instituto Tecnológico de Sonora.

## Author details

Jesús Álvarez-Sánchez<sup>1</sup>, Griselda Evelia Romero-López<sup>1</sup>, Sergio Pérez-Sicairos<sup>2</sup>, German Eduardo Devora-Isiordia<sup>1</sup>, Reyna Guadalupe Sánchez-Duarte<sup>1</sup> and Gustavo Adolfo Fimbres-Weihs<sup>3\*</sup>

\*Address all correspondence to: [gustavo.fimbres@itson.edu.mx](mailto:gustavo.fimbres@itson.edu.mx)

1 Departamento de Ciencias del Agua y Medio Ambiente, Instituto Tecnológico de Sonora, Cd. Obregón, Sonora, México

2 Instituto Tecnológico de Tijuana, Tijuana B.C., Mexico

3 CONACYT-ITSON, Departamento de Ciencias del Agua y Medio Ambiente, Instituto Tecnológico de Sonora, Cd. Obregón, Sonora, México

## References

- [1] Le NL, Nunes SP. Materials and membrane technologies for water and energy sustainability. *Sustainable Materials and Technologies*. 2016;**7**:1-28. <http://dx.doi.org/10.1016/j.susmat.2016.02.001>
- [2] Ray C, Jain R. *Drinking Water Treatment Technology—Comparative Analysis*. Dordrecht: Springer ; 2011. DOI: 10.1007/978-94-007-1104-4\_2. ISBN: 978-94-007-1103-7
- [3] Llenas L, Martinez-Llado X, Yaroshchuk A, Rovira M, de Pablo J. Nanofiltration as pretreatment for scale prevention in seawater reverse osmosis desalination. *Desalination and Water Treatment*. 2012;**36**:310-318. DOI: <https://doi.org/10.5004/dwt.2011.2767>
- [4] Carrero-Parreño A, Onishi VC, Salcedo-Díaz R, Ruiz-Femenia R, Fraga RE, Caballero JA, Reyes-Labarta JA. Optimal pretreatment system of flowback water from shale gas production. *Industrial and Engineering Chemistry Research*. 2017;**56**:4386-4398. DOI: 10.1021/acs.iecr.6b04016
- [5] Nguyen T, Roddick FA, Fan L. Biofouling of water treatment membranes: A review of the underlying causes. *Monitoring Techniques and Control Measures*. *Membranes*. 2012;**2**:804-840. DOI: 10.3390/membranes2040804
- [6] Suwarno SR, Hanada S, Chong TH, Goto S, Henmi M, Fane AG. The effect of different surface conditioning layers on bacterial adhesion on reverse osmosis membranes. *Desalination*. 2016;**387**:1-13. <http://dx.doi.org/10.1016/j.desal.2016.02.029>
- [7] Al Ashhab A, Sweity A, Bayramoglu B, Herzberg M, Gillor O. Biofouling of reverse osmosis membranes: Effects of cleaning on biofilm microbial communities, membrane performance, and adherence of extracellular polymeric substances. *Biofouling*. 2017;**33**(5):397-409. DOI: 10.1080/08927014.2017.1318382

- [8] Food and Drug Administration. Code of Federal Regulations. Title 21, Volume 2. Revised as of April 1, 2017. United States of America. ISBN: 978-1-68388-080-6
- [9] Rodríguez-Maturino A, Troncoso-Rojas R, Sánchez-Estrada A, Daniel González-Mendoza D, Ruiz-Sánchez E, Zamora-Bustillos R, Ceceña-Durán C, Grimaldo-Juárez O, Aviles-Marina M. Efecto antifúngico de extractos fenólicos y de carotenoides de chiltepín (*Capsicum annum* var. *glabriusculum*) en *Alternaria alternata* y *Fusarium oxysporum*. *Revista Argentina de Microbiología*. 2015;**47**(1):72-77. <http://dx.doi.org/10.1016/j.ram.2014.12.005>
- [10] Omolo MA, Wong ZZ, Mergen AK, Hastings JC, Le NC, Reiland HA, Case KA, Baumler DJ. Antimicrobial properties of chili peppers. *Department of Food Science and Nutrition*. 2014;**2**:145-152. DOI: 10.4172/2332-0877.1000145
- [11] Omidvar M, Soltanie M, Mousavi SM, Saljoughi E, Moarefian A, Saffaran H. Preparation of hydrophilic nanofiltration membranes for removal of pharmaceuticals from water. *Journal of Environmental Health Science & Engineering*. 2015;**13**(42):1-9. DOI: 10.1186/s40201-015-0201-3
- [12] Mitrouli ST, Karabelas AJ, Isaias NP, Rammah AS. Application of hydrophilic macromolecules on thin film composite polyamide membranes for performance restoration. *Desalination*. 2011;**278**:105-116. DOI: 10.1016/j.desal.2011.05.014
- [13] Wu D, Liu X, Yu S, Liu M, Gao C. Modification of aromatic polyamide thin-film composite reverse osmosis membranes by surface coating of thermo responsive copolymers P(NIPAM-co-Am). I: Preparation and characterization. *Journal of Membrane Science*. 2010;**352**:76-85. DOI: 10.1016/j.memsci.2010.01.061
- [14] Pérez-Sicairos S, Miranda-Ibarra SA, Lin-Ho SW, Álvarez-Sánchez J, Pérez-Reyes JC, Corrales-López KA, Morales-Cuevas JB. Nanofiltration membranes, prepared via interfacial polymerization, doped with ZnO nanoparticles: Effect on performance. *Revista Mexicana de Ingeniería Química*. 2016;**15**(3):961-975. <http://rmiq.org/iqfvp/Pdfs/Vol.%2015,%20No.%203/Poli1/RMIQTemplate.pdf>
- [15] Lin SW, Pérez-Sicairos S, Félix-Navarro RM. Preparation, characterization and salt rejection of negatively charged polyamide nanofiltration membranes. *Journal of the Mexican Chemical Society*. 2007;**51**(3):129-135 <http://www.scielo.org.mx/pdf/jmcs/v51n3/v51n3a1.pdf>
- [16] Pavia DP, Lampman GM, Kriz GS, Vyvyan JR. *Introduction the Spectroscopy*. 4th ed. USA: Cengage Learning; 978-0-495-11478-9